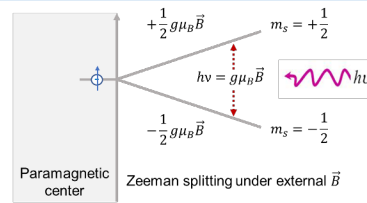


Motivation

- c-Si based solar cell efficiencies are approaching over 26%^{1,2}
- Critical to characterize the low concentration performance limiting defects – as low as 10^{10} - 10^{11} cm⁻³ (e.g., Fe contamination in GaCz Si³)
- Atomistic level understanding of the mechanisms of the low-concentration process-induced-defects and reliability limiting defects is needed (e.g., LeTID)
- Lifetime spectroscopies can still be used; however, they are based on estimations and theoretical models, and cannot fully reveal information about microscopic mechanisms.

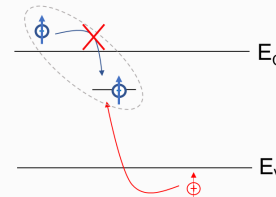
[1] Lin, H. et al., *Nat Energy* (2023) doi:10.1038/s41560-023-01255-2.
 [2] Richter, A. et al., *Nat Energy* 6, 429–438 (2021).
 [3] Basnet, R. et al., *Solar RRL* (2023) doi:10.1002/solr.202300304.

Electrically detected magnetic resonance (EDMR) principle



- Change in the cell output is due to change in the recombination at magnetic resonance condition.
- EDMR is specific and sensitive to the performance affecting paramagnetic defects.

- ✓ Spin-polarization under external \vec{B}
- ✗ No microwave radiation
- ✗ No magnetic resonance
- ✗ No spin flip
- ✗ Transition permutation equilibrium (governed by spin-selection rules)



- ✓ Spin-polarization under external \vec{B}
- ✓ Microwave radiation
- ✓ Magnetic resonance
- ✓ Spin flip
- ✓ Transition permutation equilibrium gets shifted

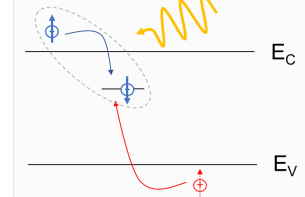
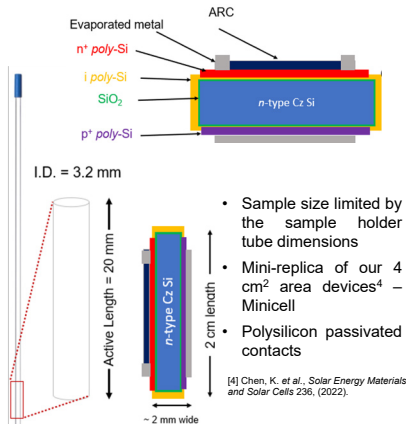


Fig. 1. (a) Zeeman-splitting; (b) Recombination under external \vec{B} ; (c) Change in recombination transitions at magnetic resonance condition.

Sample preparation



- Sample size limited by the sample holder tube dimensions
- Mini-replica of our 4 cm² area devices⁴ – Minicell
- Polysilicon passivated contacts

[4] Chen, K. et al., *Solar Energy Materials and Solar Cells* 236, (2022).

Fig. 2. (a) Cell-design; (b) Sample holder tube dimensions.

Minicell fabrication process flow

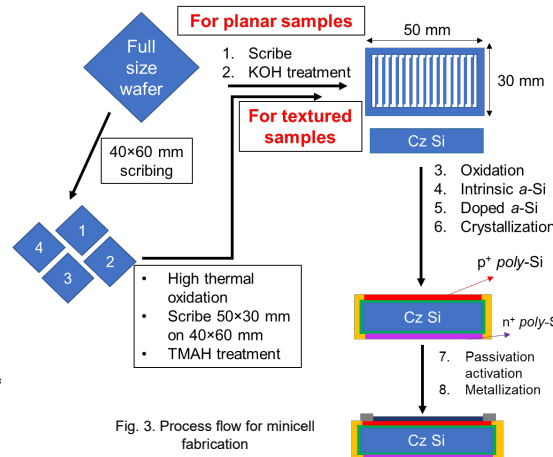


Fig. 3. Process flow for minicell fabrication

Edge ablation damage removal for edge passivation

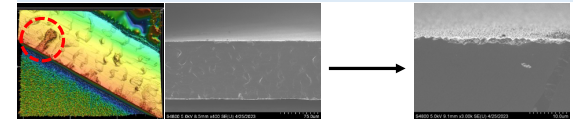
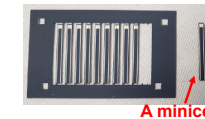


Fig. 4. Microscope images of edge of the minicell before and after ablation damage removal.

Results – Proof of concept minicells

Sample ID	V _{oc} (V)	FF	J _{sc} (mA/cm ²) (without ARC nitride)	Efficiency
Minicell-1	0.6494	74.8	25.62	12.4 %
Minicell-2	0.6598	74.7	26.24	12.9 %
4 cm ² device-1	0.6786	76.5	28.62	14.9 %
4 cm ² device-2	0.6842	76.5	28.46	14.9 %



- Performance of the minicells comparable to 4 cm² devices fabricated simultaneously

Results – Proof of concept EDMR measurements at NREL

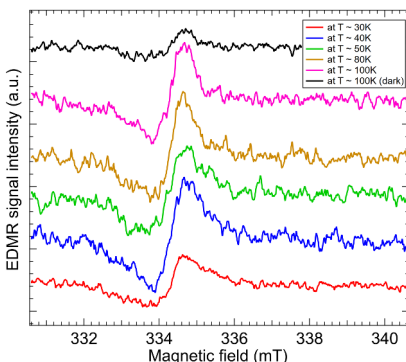


Fig. 6. EDMR measurements at temperature - 30K, 40K, 50K, 80K, 100K.

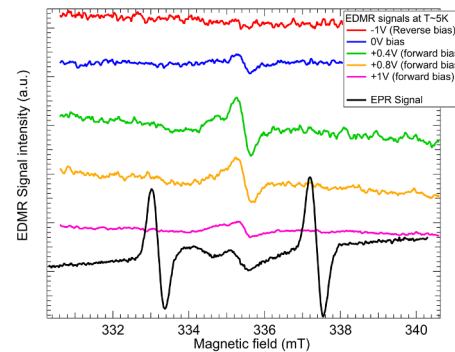


Fig. 7. EDMR measurements at temperature ~5K varying the bias

- g -value ~ 2.005 signal at likely due to the Si dangling bond inside the device at
- g -value ~ 1.998 signal at T \sim 5K temperature shows bias dependency

Conclusion

- We have shown proof of concept of minicell fabrication and EDMR measurement capability on them at NREL.
- We recorded EDMR signals at g -value ~ 2.005 and ~ 1.998 at different parameters, however, dependency of such parameters to study different recombination channels on the same device using EDMR needs to be understood properly.
- We aim to study some of the unknown defects in ongoing experiments.

Acknowledgement

This work was supported by the U.S. Department of Energy under Contract No. DE-AC36-08GO28308 with Alliance for Sustainable Energy, LLC, the Manager and Operator of the National Renewable Energy Laboratory. Funding provided by U.S. Department of Energy Office of Energy Efficiency and Renewable Energy Solar Energy Technologies Office under Agreement Number 38526. Authors also acknowledge the contribution by Prof. Dr. Klaus Lips and his students from Helmholtz-Zentrum Berlin for helping during development of EDMR instrumentation at NREL.

30th NREL Silicon Workshop 2023, Breckenridge, Colorado, USA